JOURNAL OF MATERIALS SCIENCE **38** (2003) 2581–2590

Quantitative analysis of the effect of the binder phase composition on grain growth in WC-Co sintered materials

V. CHABRETOU*, C. H. ALLIBERT, J. M. MISSIAEN
Laboratoire de Thermodynamique et de Physico-Chimie Métallurgiques, UMR 5614 CNRS-INPG/UJF, F-38402 SAINT-MARTIN D'HERES Cedex
E-mail: missiaen@ltpcm.inpg.fr

Microstructural evolution of WC-Co materials with different compositions and WC grain sizes is discussed from SEM observations and quantitative image analyses of intercept length distributions in the WC phase. Effect of the C/W ratio in the binder phase and of V- or Cr-dopants is particularly studied. Microstructural coarsening is shown to be more rapid and less abnormal when the C/W ratio is increased in the two-phase field {WC + liquid} and up to the three-phase field {WC + C + liquid}. The V-dopant does not completely suppress this effect. The composition dependence of the liquid stability—analysed from the calculated Gibbs energies of the phases—could explain the trend of the experimental results.

1. Introduction

The cemented carbides WC-Co are typically used as drilling or cutting tools and wear resistant tools because of their excellent hardness and strength. These materials consist of an homogeneous distribution of faceted WC grains embedded in a Co-based binder. The reduction of the WC grain size results in enhanced mechanical properties. Materials are processed from WC and Co powders by liquid phase sintering (LPS) at about 1300–1500°C. At sintering temperature, grain growth of WC grains in the Co-based liquid can occur [1–3]. Such a microstructure evolution is detrimental to the properties and can be limited by the addition of some elements such as V or Cr that inhibit grain growth [4, 5]. The parameters of the sintering process with or without inhibitors are numerous and the process optimisation is difficult. Obviously, the initial WC particle size, that determines the driving force for grain growth, is the major parameter. Another main factor is the binder composition: at sintering temperature, the composition field of the ternary Co-based liquid in equilibrium with WC extents for values of C/W ratio from about 2.8 to 0.6. Small amounts of graphite (C) or η phase (Co_3W_3C) can form for values higher or lower than these limit ratio.The literature results evidence an effect of the carbon content. Except Wu and co. [6] who have related a reduction of grain growth rate to an increase in C content, most authors [7–10] noticed that the WC grain size is larger in a C-rich binder. This trend was also observed in a preliminary study by the present authors [11] and the investigation carried out in parallel works by Transmission Electron Microscopy (TEM) showed that microstructural features—morphology of the WC grains and WC/Co interfaces—acting on crystal growth are different in C-rich and in W-rich or Cr-doped alloys [12, 13]. However, if the literature often reports an enhancement of WC grain growth by a C content increase in the binder phase, it rarely provides a quantification of this effect.

The purpose of the present study was a more precise determination of the effect of the binder composition on the evolution of the WC particle population at sintering temperature. The influence of the C/W ratio in the binder phase, of the presence of a C or η phase and of the addition of V or Cr was examined in materials prepared from WC powder with "coarse" (5.5 and 1.7 μm) and "fine" (0.9 μm) initial median sizes.

2. Experimental procedure

2.1. Studied materials and specimens preparation

The published results, while somewhat contradictory, indicate a small influence of the binder fraction on the microstructure evolution in WC-Co [6, 7, 14–16]. Consequently, the microstructure evolution can be investigated in {WC + liq} mixtures with large liquid fractions which are still representative of the sintered materials. Quantitative analysis of the WC microstructure and control of the binder composition are then easier.

**Present address*: ASCOMETAL CREAS, BP70045, 57601 Hagondange Cedex, France.

TABLE I Compositions of the samples, in at.%, Co balance

	C	W	V	Cr
(1)	25.5	25	0	0
(1)V	26.5	25	1.5	0
(2)	25	28	0	0
(2)V	25	28	1.5	0
(3)	30	20	0	0
(3)V	30	20	1.8	0
(3)Cr	30	20	0	1.8
(4)	20	30	0	0
(4)V	20	30	1.8	0
(4)Cr	20	30	0	1.8
(1S)	43.35	43.25	0	0
(1S)V	43.35	42.95	0.4	0
(2S)	42.85	43.65	0	0
(2S)V	42.95	43.25	0.4	0

Six ternary alloys were studied. Their compositions are given in Table I and reported on the section at 1425°C determined by Akesson [17] (Fig. 1). At this temperature, four alloys (1), (2), (1S) and (2S) are in the two-phase field {WC + liq}. The compositions (1) and (1S) are on the line WC-$Co_{0.99}C_{0.01}$, the alloys (2) and (2S) are on the line WC-$Co_{0.94}W_{0.06}$.The Co contents are about 35 wt% in (1), (2) and 8 wt% in (1S) and (2S). The compositions (3) and (4) are respectively located in the three-phase domains {WC + liq + C} and {WC + liq + η}. Eight quaternary alloys, with a small amount of V or Cr, were investigated. Their compositions correspond to about 3 at.% Co substituted for the inhibitor in the ternary binders. Such an amount was deduced from the V (or Cr) content in industrial grades, on the basis that V (or Cr) is dissolved in the binder as shown elsewhere [18]. At 1450°C, the volume fractions of liquid, calculated from different data [19], are about 19% in (1S) and (2S), and 67% in (1), (2) and (3). The composition (4) corresponds to 55 vol% of liquid and 25 vol% of η, the formation of which requires a significant dissolution of WC.

Specimens were prepared by mixing Co and WC powders, plus C, W, VC or Cr_3C_2 powders if necessary. WC powders with median sizes 5.5, 1.7 and 0.9 μm, and maximum sizes 50, 12 and 8 μm (from Laser Diffraction measurements), were used as starting materials. The mean grain size of the other powders was around 1 μm. The most important impurity in the powders is oxygen with a content around 1000–3000 ppm. After mixing without lubricant for 1 h in a "turbula" mixer, the powders were compacted at 600 MPa. The compacts were heat treated at 900°C for 1 h under hydrogen flow to reduce the oxygen level, then at 1450°C or 1600°C under static Ar atmosphere for 0 to 9 h. The heating rate was about 70 K/min until 1200°C, and 20 K/min above. All samples were furnace cooled, at about 85 K/min. After sintering, the oxygen content, checked by chemical analysis, was less than 250 ppm. The notations and characteristics of the studied alloys are grouped in Table II.

TABLE II Compositions, WC size and heat treatments. The specimens will be named by their composition, the introduced inhibitor and the WC powder size. For example, (1)V-5.5 stands for the sample of composition (1), with vanadium and prepared with WC powder of 5.5 μm median size

	(1)	(2)	(3)	(4)	(1S)	(2S)
ϕ_{WC}(μm)	5.5–1.7	5.5–1.7	5.5–0.9	5.5–0.9	1.7	1.7
Inhibitor	V	V	V-Cr	V-Cr	V	V
T(°C)	1450	1450	1450–1600	1450–1600	1450	1450

2.2. Characterisation techniques

Quantitative metallographic analysis was performed on polished vertical sections. Murakami etching during 30 s—10 wt% KOH and $K_3Fe(CN)_6$—was used when the η phase was present. To get statistical results, a uniform sampling was done on sections, and 20 images were acquired by scanning electron microscopy (SEM, Leo Stereoscan 440) in the backscattered mode. The accelerating voltage was fixed at 10 kV to limit the penetration depth of the electrons. Aphelion image analysis software (ADCIS) was used for the image treatments and measurements. Grey-tone images were thresholded to get binary images of the WC phase. The mean intercept lengths, volume-weighted intercept length distributions and the covariance functions were systematically measured on the WC phase, without separating WC grains, using standard automatic image analyses [20, 21]. Evolution of the mean intercept length, and of the intercept length distribution is then significant of a

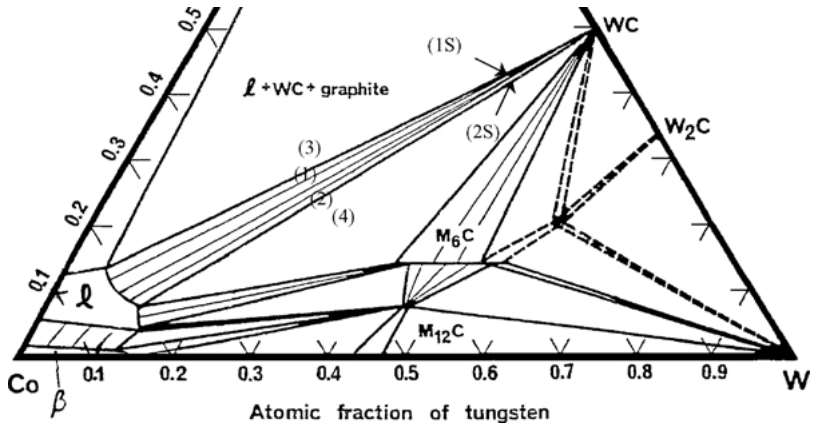

Figure 1 Compositions of the studied ternary alloys reported on the equilibrium phase diagram at 1425°C (from [17]).

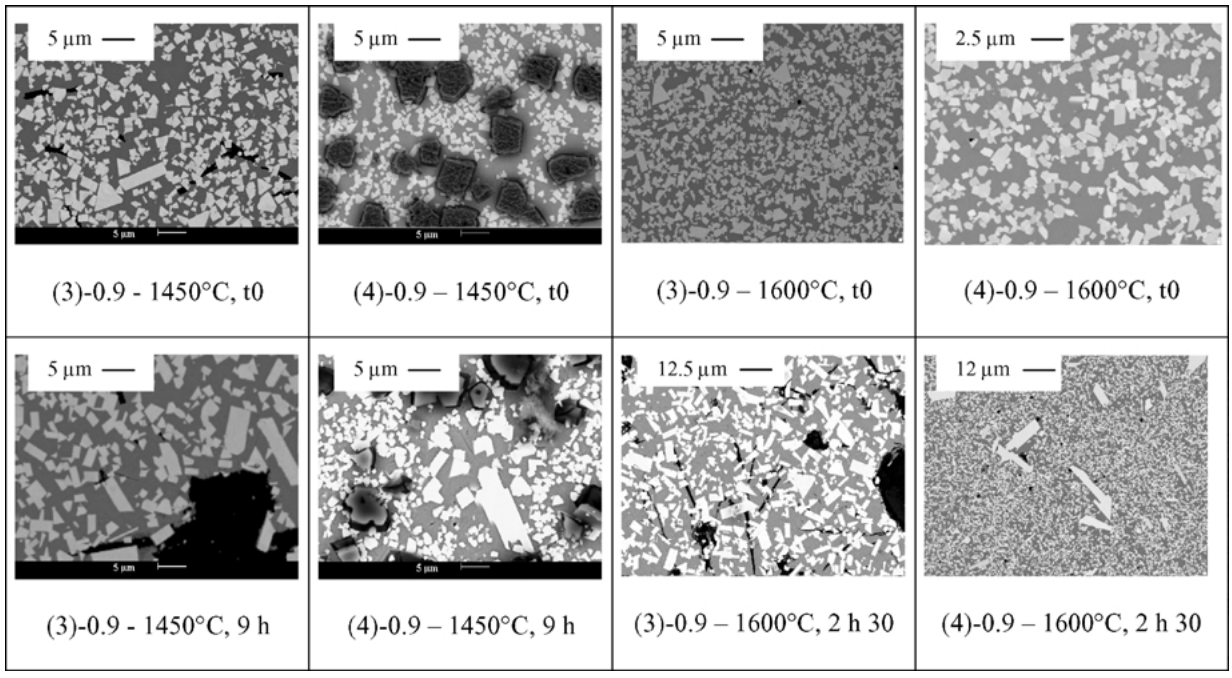

Figure 2 SEM micrographs of samples (3)-0.9 and (4)-0.9. (WC in white, Co in grey, η in dark grey and C in black).

grain size evolution only if the contiguity of the WC phase does not vary, which means in particular that the volume fraction does not vary. Variation of contiguity with sintering time at 1450°C has been quantified for samples (1)-1.7 by separating WC grains on the images. No significant variation was detected. Contiguities of samples (1)-5.5 and (1)V-5.5 have also been compared, showing no significant effect of the V-doping on contiguity. A slight decrease of contiguity with sintering time at 1450°C was however quantified for alloys with submicronic particles ($\Phi_{WC} = 0.9\ \mu$m). In that case, the variation of the mean intercept length due to grain growth would have been higher if separation of the grains had been performed. The intercept lengths are number-weighted averages,whereas intercept lengths presented in a previous paper [11] were obtained by averaging the volume-weighted distributions.

3. Results

3.1. Microstructural features

Typical microstructures of alloys with a large Co fraction prepared with submicronic WC powders are compared on Figs 2 and 3. In ternary alloys (Fig. 2), abnormal WC grains larger and more anisotropic than most of the "matrix" grains are present at long sintering time. The difference in size and anisotropy between the abnormal and matrix grains is larger in the W-rich than in C-rich samples. In alloys containing Cr or V (Fig. 3), the microstructure is homogeneous and finer, and no "abnormal" grains are detected in the conditions presently used.

When the binder is enriched in C, WC grains are faceted. In the W-rich or in V-doped alloys, some WC grains appear slightly rounded. This loss of facets was already noticed by Shi and Matsubara [22] from SEM observations at higher magnification. It was shown by Wang *et al*. [12, 13] from TEM observations to correspond to rounding of WC grain corners and formation of small steps on the basal and prismatic planes of WC crystals. At the step edge, small precipitates of the cubic phase (V, W)C are detected [18] in the V-doped alloys.

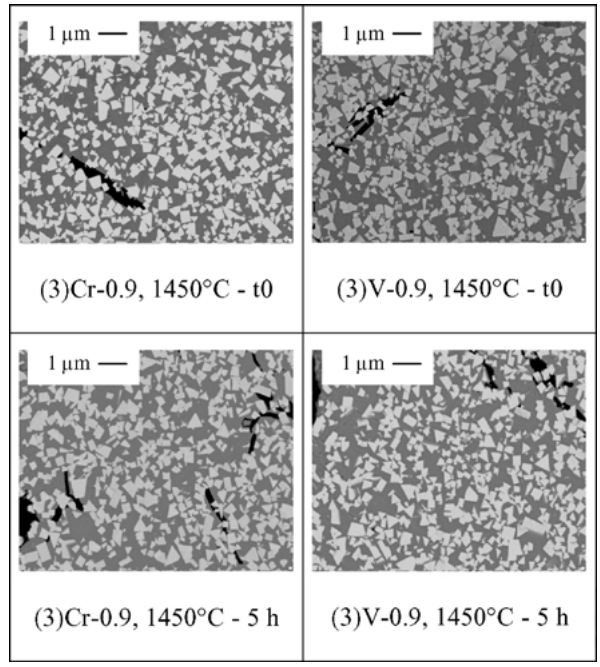

Figure 3 SEM micrographs of samples (3)Cr-0.9 and (3)V-0.9. (WC in white, Co in grey and C in black).

In the three-phase specimens with a large liquid fraction, a binder film is often detected between WC and η grains, whereas graphite and WC seem in contact. This indicates that the interface energy is higher between WC and η than between WC and liquid, and WC and graphite.

The stable η-β and the metastable η-β-C eutectic structures are often observed in the binder, as mentioned previously [18]. They indicate the easier nucleation for C or η phase than for WC.

No sedimentation of the WC phase, much denser than the Co binder, is observed even in the specimens with the larger liquid fraction and coarse WC size: this indicates the continuous 3D network formed by the WC particles.

3.2. Homogeneity and anisotropy

The statistical errors on intercept measurements are less than 1.5%, and the covariance function reaches its asymptotic plateau for a size smaller than the size of the images, indicating that the microstructure is homogeneous. Measurements of the mean intercept lengths and of the covariance functions in two perpendicular directions show very close values, and do not detect any anisotropy of the microstructure.

3.3. Size evolution for materials prepared with coarse WC powders

For materials prepared with WC powder sizes 5.5 and 1.7 μm, the mean intercept lengths at the beginning, and after 5–6.5 h at 1450°C, are compared for the different compositions (Fig. 4a and b). Whatever the composition, the effect of sintering time on the mean intercept is weak for WC powder 5.5 μm. In materials prepared with WC 1.7 μm, grain growth is more visible in the ternary alloys with 8 wt% Co and is slightly more pronounced in the C-rich than in W-rich binder.

In fact, the major differences are observed between mean intercepts measured at the beginning of sintering. The initial mean intercepts in samples with 8 wt% Co are larger than in the corresponding compositions with 35 wt% Co, which is expected, since the volume fraction of the WC phase, and therefore the contiguity, is then higher. In the ternary two-phase alloys, the initial intercepts are very similar for composition (1) and (2), both for WC powder size 5.5 μm and 1.7 μm. In the three-phase alloys, the initial intercept in (3)-5.5 is close to that in the ternary alloys (1) or (2) but is smaller in (4)-5.5. This difference can be related to the dissolution of WC grains to form η phase, which reduces both the size and volume fraction of the grains. The addition

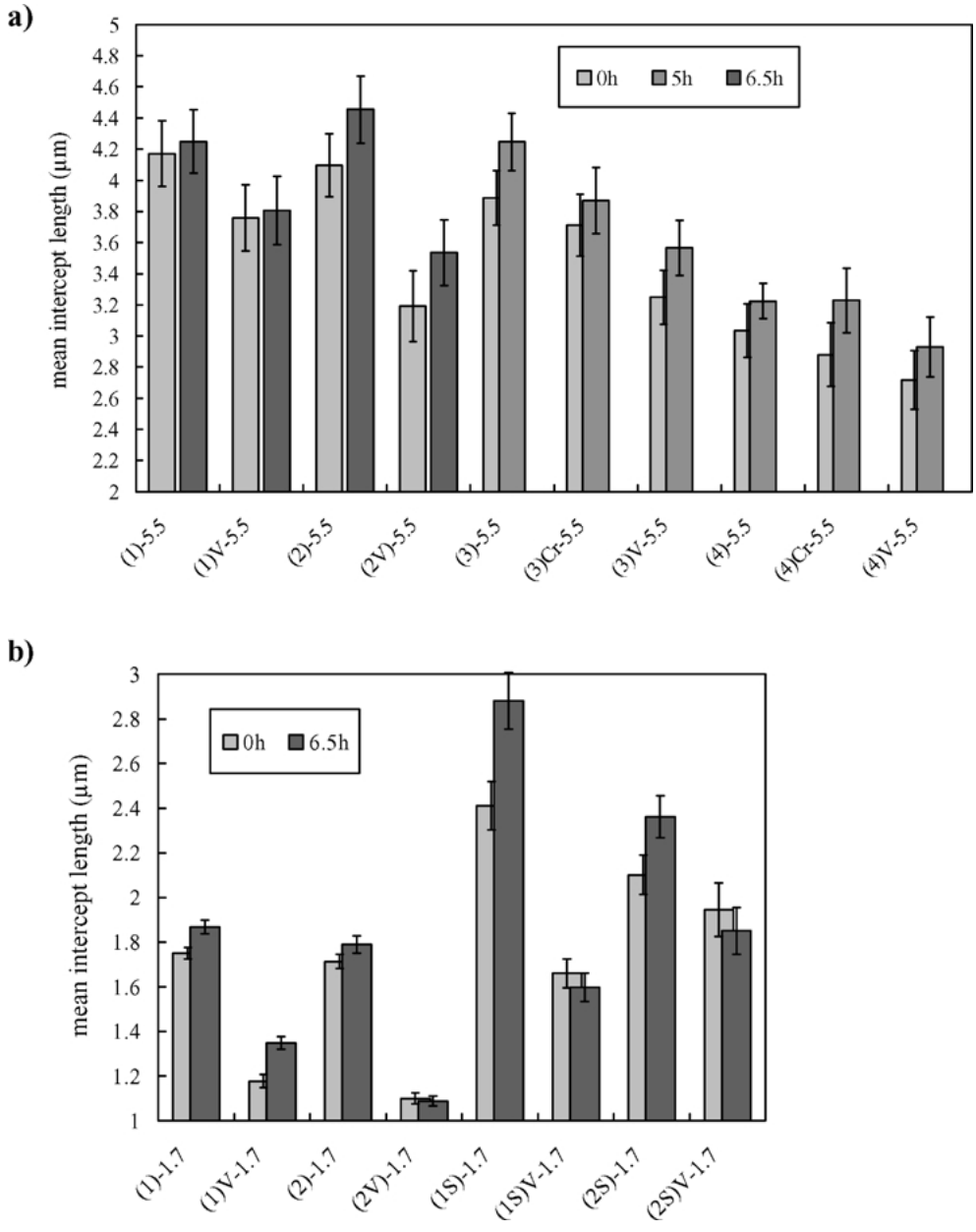

Figure 4 Mean intercept lengths at the beginning and after 5–6.5 h sintering at 1450°C: (a) $\phi_{WC} = 5.5$ μm and (b) $\phi_{WC} = 1.7$ μm.

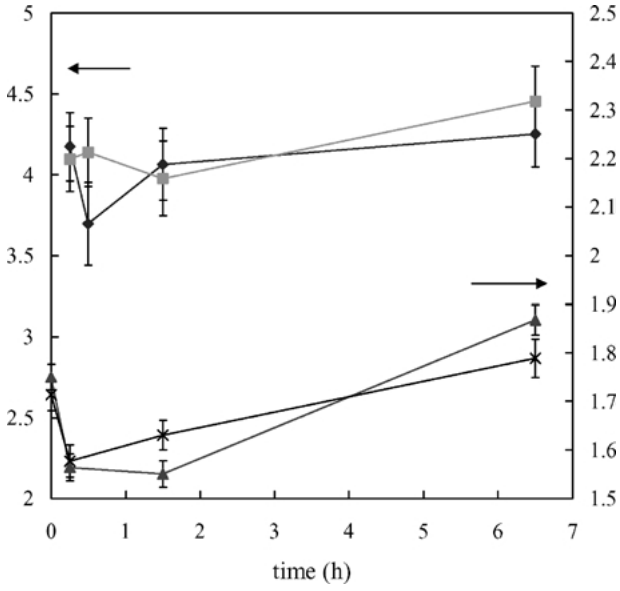

Figure 5 Mean intercept versus sintering time. $\phi_{WC} = 5.5\ \mu$m: ◆ (1)-5.5, ■ (2)-5.5, $\phi_{WC} = 1.7\ \mu$m: ▲ (1)-1.7, × (2)-1.7.

of Cr or V produces a decrease of the initial mean intercepts of the ternary alloys, higher with V than with Cr.

In the ternary two phase alloys, a more detailed study of the time dependence of the mean intercepts detects a small decrease after 1 h 30 (Fig. 5). While this decrease is in the confidence interval for the samples prepared with the 5.5 μm powder, it is found significant in the samples with same compositions, prepared with the 1.7 μm powder. Different phenomena—penetration of Co into WC agglomerates, evolution of the grain shape or of the size distribution—might explain this decrease.

The intercept distributions are asymmetric. Their features—peak close to the small intercepts, long tail for large intercepts—are similar to those described below for submicronic materials.

3.4. Size evolution for materials prepared with submicronic WC powder

The variation of the WC mean intercept with sintering time is shown Fig. 6 for the alloys prepared with the fine WC powder (0.9 μm). The growth rate is larger in the (WC-liquid-C) than in (WC-liquid-η) field. As expected, the growth is not detectable in V or Cr containing mixtures. The mean intercept is smaller in the quaternary than in the ternary alloys. For a given C/W ratio in the ternary alloys, the mean intercept reduction is higher with vanadium than with chromium addition.

The variation of the intercept length distributions with sintering time (Fig. 7) is associated to a significant evolution of the distribution of the reduced intercepts l/l_{mean}, even after a few hours (Fig. 8): the maximum reduced size l_{max}/l_{mean} increases while the distribution peak tightens. The evolution of l_{max}/l_{mean} characterises the "abnormal" character of the growth for the different alloys.

Abnormal grain growth is more pronounced on the W-rich side, as displayed by the microstructures (Fig. 2), showing the formation of large grains, while most of the grains hardly evolve if at all. The difference between the W-rich and C-rich alloys is enhanced at higher sintering temperature. It is difficult to quantify at 1450°C (Fig. 9a), because only few WC grains have grown in W-rich samples, so that none of them has been taken into account by the uniform sampling. It is well evidenced at 1600°C. The intercept length distribution is then more asymmetric, with a tighter peak and a larger maximum intercept in W-rich than in C-rich samples (Fig. 9b). The intercept length distributions of samples with inhibitor are slightly less asymmetric with a shorter tail (Fig. 10).

4. Discussion

The size distribution analysed here is the intercept length distribution in the WC phase, without separation of the grains. Although this distribution cannot be directly related to the grain size distribution of the 3D polyhedral particles, its evolution is expected to represent qualitatively the basic trends of the evolution of the 3D grain size distribution as far as the volume fraction is fixed, if both the particle shape and contiguity do not vary too much. Moreover, a self-similar evolution of the microstructure should yield a stationary size distribution in reduced size units, whatever the size distribution.

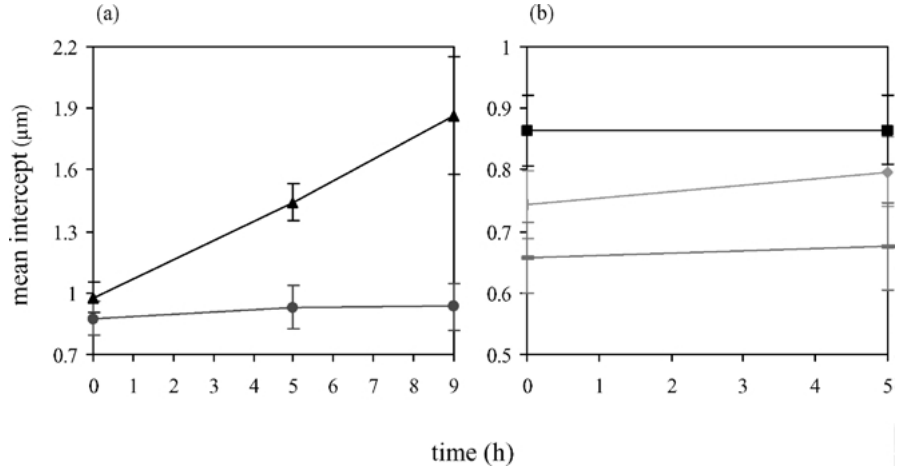

Figure 6 Mean intercept versus sintering time (ϕ_{WC} = 0.9 μm). (a) ternary alloys: ▲ (3)-0.9, ● (4)-0.9, (b) quaternary alloys : ◆ (3)V-0.9, ■ (4)Cr-0.9, – (4)V-0.9.

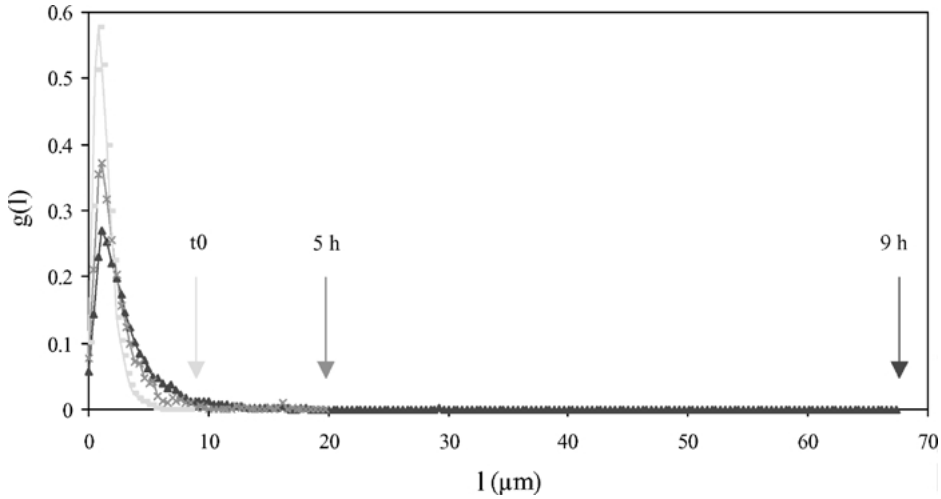

Figure 7 Variation of the (3)-0.9 intercept length distribution versus sintering time. - t0, x 5 h, ▲ 9 h.

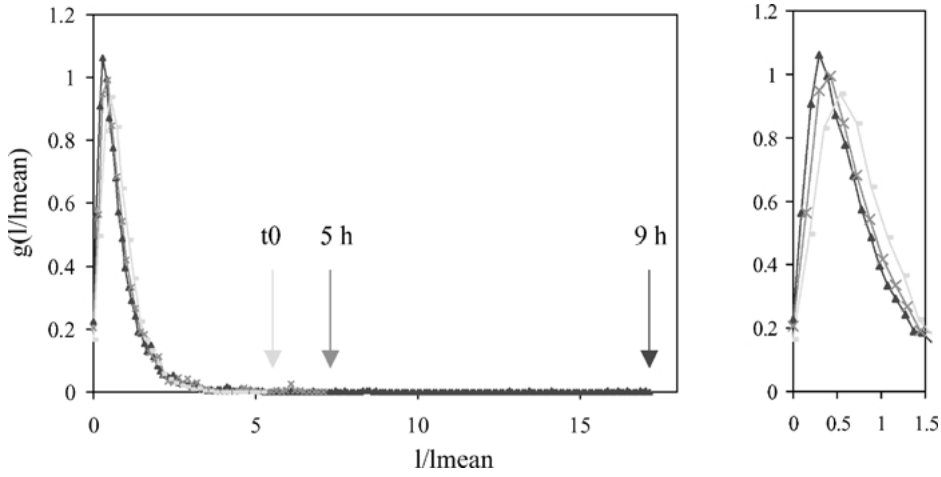

Figure 8 Variation of the reduced intercept length distributions for the (3)-0.9 alloy. - t0, x 5 h, ▲ 9 h.

Hence, the intercept analysis can be used to evidence any abnormal character of grain growth.

The driving force for the growth of WC grains in a Co-based liquid is the reduction of the WC/liquid interface area. Obviously, the smaller the initial WC grain size, the larger the interface area and the larger the driving force. The present results confirm the expected effect of the WC grain size on the microstructure variation. For WC particles with size around or below 1 μm, the "abnormal" growth is evidenced by the un-stationary variation of the reduced intercept length distribution with sintering time, even after a few hours (Fig. 8). For WC grain sizes above 1 μm as reported in the literature [14, 23], the growth rate is extremely small, and the un-stationary evolution is not detectable.

The results also emphasise the major contribution of the C/W ratio in the binder phase: both the initial mean intercept and the mean intercept variation are smaller in ternary alloys with a lower C/W ratio, and/or in doped materials. This can be explained by the enhancement of grain growth during heating and during isothermal holding as the carbon content increases, in agreement with previous quantitative analyses [7, 8]. The differences—obvious between the η and graphite sides—are slightly less pronounced in the 2-phase alloys (WC + liquid) with different C/W ratio in the liquid, and are not completely suppressed by the V or Cr additions. Other effects could contribute to the differences in mean intercepts: η phase formation during heating for the (WC-liquid-η) mixtures, which would consume part of the WC phase, and could explain a lower initial mean intercept for these alloys; slight contiguity variations, which could be different in W-rich and in C-rich alloys, and induce differences on the initial mean intercepts or on the intercept variations during isothermal holding. The intercept distribution also becomes more asymmetric in the W-rich 3-phase alloys (Fig. 9), i.e., the abnormal character of grain growth is more pronounced. A higher growth rate of large grains in W-rich alloys was also noticed by Kim *et al*. [10].

Kinetics of grain growth in WC-Co materials are classically postulated to be limited by a reaction step [14, 23, 24]. This reaction would involve a 2D-nucleation or a defect-assisted nucleation step, which could explain the abnormal character of grain growth [1]. In the present work, the large interface area required to provide the critical driving force to start grain growth is consistent with kinetics limited by a nucleation step. However, the precise mechanisms of the reaction step and the role of the binder phase composition on these mechanisms are yet not clear.

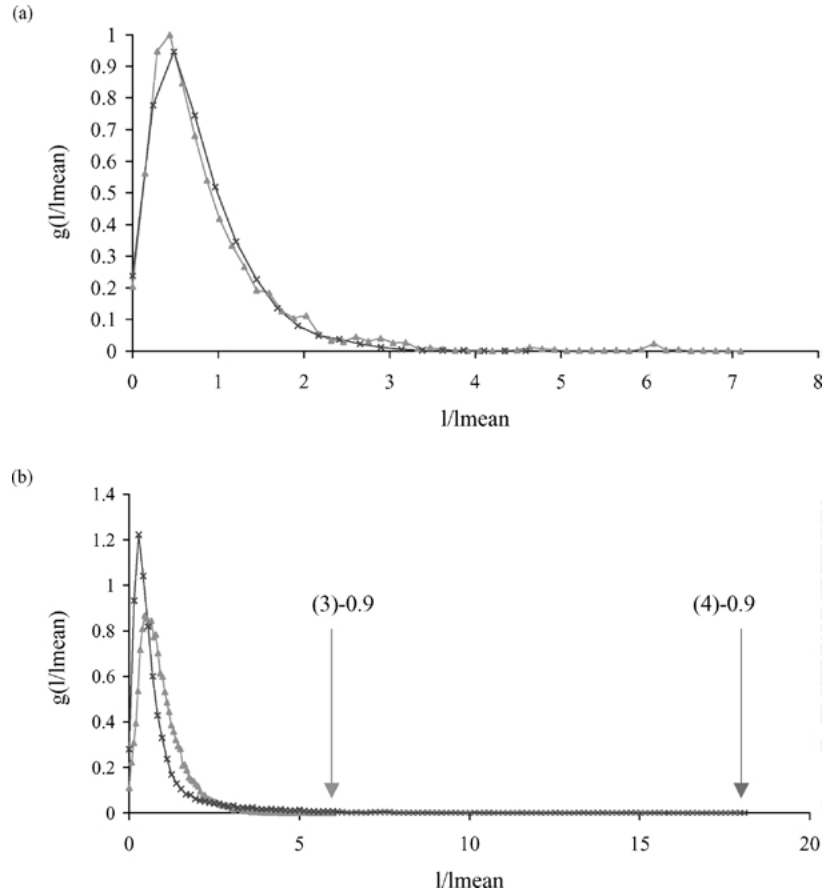

Figure 9 Comparison of the reduced intercept length distributions for the alloys ▲(3)-0.9 and × (4)-0.9. (a) 1450°C, 5 h and (b) 1600°C, 2 h 30.

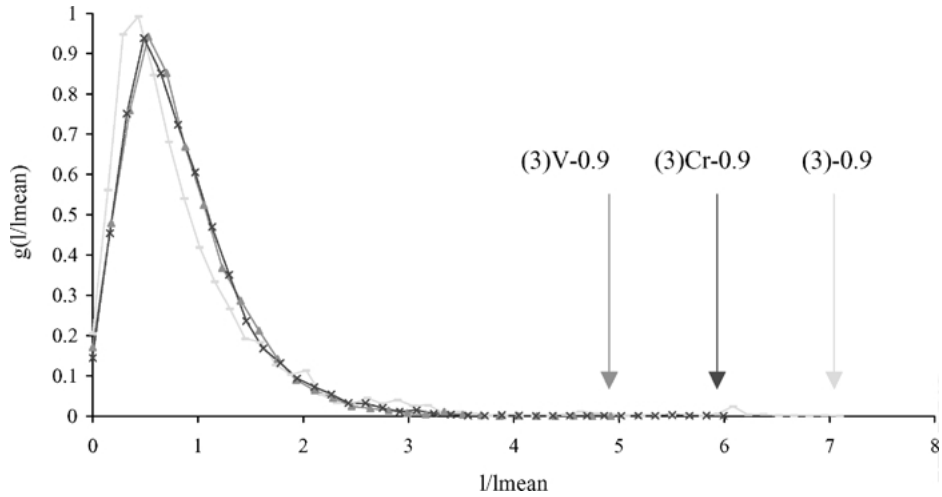

Figure 10 Comparison of the reduced intercept length distributions for the alloys - (3)-0.9 ▲ (3)V-0.9 and × (3)Cr-0.9, 1450°C, 5 h.

To know if the composition effect may have a thermodynamic origin, the stability of the different phases (liquid, WC, graphite and η) was considered from the Gibbs energies G calculated from the data of [17] at 1450°C. For the ternary liquid, the Gibbs energy G_L is represented by a 3-D surface. An easier visualisation of the composition dependence of G_L is given by the 2D-curves of iso-G_L values reported on the isothermal section (Fig. 11a). The data show a significant composition effect. In the direction of WC or W_2C, the iso-G_L sections are larger and separated by longer distances: the liquid stability is higher on the side of WC and W_2C and lower towards C. The formation of the metastable equilibrium {liquid + C + η} in cooling conditions—rather than the stable equilibria {liquid + WC + η} and {liquid + WC + C}—is likely due to (i) the nucleation-growth of η, easier than that of WC [25] and (ii) the C precipitation promoted by the lower liquid stability towards C, while the nucleation-growth is known to be difficult for C as for WC. The extension of the calculated liquid domain in the direction of WC for the metastable equilibria involving liquid, C and η (Fig. 11) displays the same trend.

The composition dependence of G_L could affect the driving force available for the precipitation of WC from the liquid supersaturated by the grain size effect. As

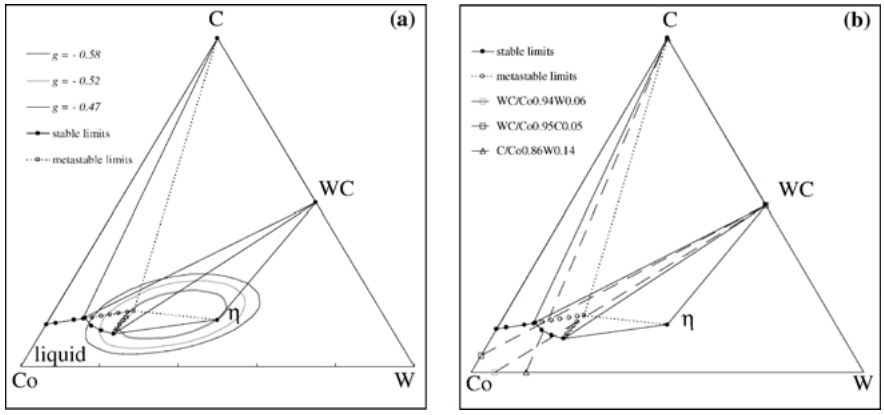

Figure 11 (a) Ternary W-C-Co phase diagram showing cuts of iso-Gibbs energy of the liquid calculated at 1450°C from the data of Akesson [17] for different values of $g = \Delta G/RT$ and limits of the stable and metastable phase fields calculated using the software "Melange" [39]. (b) position of the composition lines in the stable field {WC + liquid} and in the metastable field {C + liquid}which were used for vertical section plots of Fig. 12.

shown by Hillert [26], the driving force available for the precipitation of the WC phase is related to the difference between the Gibbs energies $G_{\mathrm{L}}^{\mathrm{s}}$ of the supersaturated liquid and $G_{\mathrm{M}}^{\mathrm{e}}$ of the equilibrium mixture {liquid + WC} for the same composition $x_{\mathrm{L}}^{\mathrm{s}}$ of the liquid:

$$\Delta G_{\mathrm{p}} = \left(G_{\mathrm{M}}^{\mathrm{e}} - G_{\mathrm{L}}^{\mathrm{s}}\right) \quad \text{at } x_{\mathrm{L}} = x_{\mathrm{L}}^{\mathrm{s}} \tag{1}$$

In our case, the composition $x_{\mathrm{L}}^{\mathrm{s}}$ can be calculated from the supersaturation induced by the size effect:

$$x_{\mathrm{L}}^{\mathrm{S}} = x_{\mathrm{L}}^{\mathrm{e}}\left(1 - \frac{2\gamma_{\mathrm{SL}}\Omega}{rRT}\right) \tag{2}$$

where $x_{\mathrm{L}}^{\mathrm{e}}$ is the liquid composition in equilibrium with WC, γ_{SL} the WC/liquid interfacial energy, r the particle size and Ω the molar volume.

The calculation was effected along two tie-lines in the equilibrium 2-phase field {liquid + WC} in which the quasi-binary behaviour can be considered. The studied lines correspond to an excess of W (WC-$Co_{0.94}W_{0.06}$) and C (WC-$Co_{0.95}C_{0.05}$) and represent respectively the composition (2) of the experimental study and the limit on the C-rich side. The driving force for the C precipitation was also calculated along the line {C-$Co_{0.86}W_{0.14}$} located in the quasi-binary metastable field {liquid + C} (Fig. 11b). The Gibbs energies of WC, C and the 2D-cuts of G_{L} along the studied lines are represented on Fig. 12 that also schematises the calculation principle. The size induced supersaturation was assumed similar in the three cases. The calculated driving force ΔG_{p} available for the solid phase (WC or C) precipitation at 1450°C for a supersaturation induced by a particle size of 150 nm are given in Table III. In the stable field {liquid + WC} the 2D-cuts of G_{L} are similar, however the driving force for the WC precipitation is slightly lower from the W-rich than from the C-rich liquid. In the metastable domain {liquid + C}, the driving force for the precipitation of C is much higher than that of WC. These values confirm the easier precipitation from the less stable liquid on the C-rich side.

It is difficult to evaluate if the small variations of ΔG_{p} with the binder composition effectively affect the WC

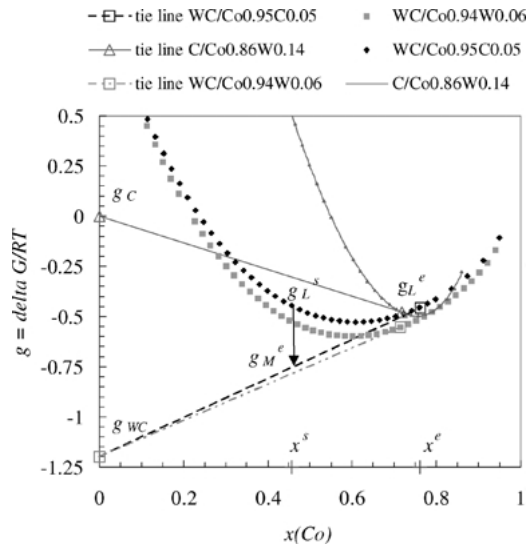

Figure 12 Gibbs energy calculated for the different phases. The curves represent the cuts of the Gibbs energy of the ternary liquid along the lines WC-$Co_{0.94}W_{0.06}$ (■), WC-$Co_{0.95}C_{0.05}$ (◆) and C-$Co_{0.86}W_{0.14}$ (▲) versus the Co content. The lines represent the Gibbs energy of the equilibrium mixtures {WC + liquid} and {C + liquid} along the corresponding tie-lines. Along the line WC/$Co_{0.95}C_{0.05}$, the driving force for the precipitation of WC from the supersaturated liquid with the Co content x^{s} is the difference $(g_{\mathrm{L}}^{\mathrm{s}} - g_{\mathrm{M}}^{\mathrm{e}})$. For a clear representation, the supersaturation $(x^{\mathrm{s}} - x^{\mathrm{e}})$ and the driving force on the figure are much more larger than those induced by the size effect.

precipitation, since the magnitude range of the energy barrier required for the WC nucleation is not known. From published experimental results [27], the supersaturation evaluated for the 3-D nucleation of a single crystal of WC in liquid Co is around 10% that corresponds, from the G_{L} values, to a nucleation energy of 300 J/mol. Much lower values are expected for the

TABLE III Calculated driving forces available for the precipitation of the solid phase WC or C at 1450°C, from the supersaturation $\Delta x \sim 10^{-3}$ induced by a grain size ~150 nm ($\gamma_{\mathrm{SL}} = 0.25$ J/m^2; $\Omega = 6.24 \times 10^{-6}$ m^3/mol $W_{0.5}C_{0.5}$—see the main text for notations)

	$WC_{precipitation}$		$C_{precipitation}$
	WC-$Co_{0.94}W_{0.06}$	WC-$Co_{0.95}C_{0.05}$	C-$Co_{0.86}W_{0.14}$
ΔG_{p} (J · mol^{-1})	2.5	4.5	12.5

2-D nucleation or for the nucleation on 2D-defects on the surface of existing WC grains. However, calculated ΔG_p values are only about 2–15 J/mol for particles of size 150 nm, and the nucleation barrier is likely to be overpassed only for high local supersaturation, locally produced by very small particles or by fluctuations of the liquid composition. Consequently, nucleation may be easier in the C-rich alloys, since local supersaturations with a higher C/W ratio are then more frequent, and the driving force for precipitation is higher when the liquid composition is enriched in C.

For liquid compositions close to the equilibrium with graphite, at a given supersaturation, the available driving force is higher for graphite than for WC precipitation which suggests that the less abnormal and more rapid grain growth could result of a mechanism involving the previous nucleation of some graphite at the WC/liquid interface.

In addition to this thermodynamic effect, the nucleation-growth mechanisms may also be composition dependent, as suggested by the WC/β interfaces, smooth on the C-rich side, with steps in the W-rich alloys. The steps at the interface WC/liquid suggest that the mechanism limiting the growth is similar in the alloys containing a Cr, V or W excess. Different phenomena are usually invoked to explain this effect of composition on the nucleation-growth mechanisms: the segregation of additives (V, Cr, W) or the precipitation of secondary carbides at the WC-Co interfaces, which would reduce the interface mobility [3, 28–32]; the formation of metal/carbon clusters in the liquid phase, which would impede liquid phase transport of W and C [33, 34]. Other mechanisms like coalescence [35, 36] or recrystallisation of defect-free grains in milled powders [37] also contribute to grain growth in WC-Co materials and may be composition dependent [38]. Work is in progress to clarify the role of composition on the mechanisms of grain growth.

5. Conclusions

The composition effects—C/W ratio and V or Cr additions in binder, compositions with Graphite or η—on the microstructure evolution of WC-Co based mixtures were studied on materials prepared from coarse (5.5 or 1.7 μm) or fine (0.9 μm) WC powders. The analysis of intercept length distributions, of microstructure and of interface morphology lead to the following conclusions:

– In agreement with the literature results, in materials prepared from coarse powders, the microstructure evolution corresponds to an extremely limited WC grain growth. The change of the reduced intercept distributions with sintering time is not detectable.

– In materials prepared from fine powders, the abnormal growth is featured by unstationary reduced intercept distributions. The increase of the maximum reduced size l_{max}/l_{mean} is related to the apparition of some anisotropic large WC grains in the fine WC grain population.

– Grain growth is slightly smaller in alloys with a W-rich binder, and significantly reduced in alloys containing η and/or V or Cr It is more anarchic and "abnormal" in the W-rich alloys, and more rapid and more homogeneous in the C-rich alloys. Cr and mainly V additions practically suppress grain growth.

– The growth rate and the morphology of the WC/liquid interfaces, different in C-rich or W-rich alloys suggest that the steps controlling the WC nucleation-growth should change with the binder composition. According to the phase stability, the nucleation activated by the graphite precipitation at WC/liquid interface is one possible cause of grain growth activation in the C-rich alloys.

Aknowledgments

The present work was financially supported by CERMeP and Sandvik Hard Materials AB. The authors wish to thank Dr B. Uhrenius form Sandvik Hard Materials, Dr S. Rimlinger and Dr E. Pauty from CERMeP for fruitful discussion and technical assistance.

References

1. Y. J. PARK, N. M. HWANG and D. Y. YOON, *Metall. Trans.* A **27** (1996) 2809.
2. A. BOCK, *Powder Metall. Int.* **24** (1992) 20.
3. K. CHOI, N. M. HWANG and D. Y. KIM, *ibid.* **43** (2000) 168.
4. K. HAYASHI, Y. FUKE and H. SUZUKI, *J. Jap. Soc. Powder & Powder Metall.* **19** (1972) 67.
5. W. D. SCHUBERT, A. BOCK and B. LUX, *Int. J. of Refractory Metals & Hard Materials* **13** (1995) 281.
6. L. WU, B. K. KIM, B. H. KEAR and L. E. McCANDLISH, in Proceedings of 13th Int. Plansee Seminar, edited by H. Bildstein and R. Eck (Plansee AG, Reutte, 1993) Vol. 3, p. 667.
7. J. GURLAND, *J. Metals* (1954) 285.
8. G. J. REES and B. YOUNG, *Powder Metall.* **14** (1971) 185.
9. H. E. EXNER, *International Metals Reviews* **24** (1979) 149.
10. S. KIM, S.-H. H. HAN, J. K. PARK and H.-E. KIM, in Proceedings of 15th Int. Plansee Seminar, edited by G. Kneringer, P. Rödhammer and H. Wildner (Plansee AG, Reutte, 2001) Vol. 2, p. 294.
11. V. CHABRETOU, J. M. MISSIAEN, C. ALLIBERT and O. LAVERGNE, in Proceedings of Powder Metallurgy World Congress (EPMA, Grenade, 1998) Vol. Special Interest Seminar: Hard Materials, p. 51.
12. Y. WANG, M. HEUSCH, S. LAY and C. H. ALLIBERT, *Phys. Status Solidi A-Appl. Res.* **193** (2002) 271.
13. Y. WANG, E. PAUTY, S. LAY and C. H. ALLIBERT, *ibid.* **193** (2002) 284.
14. J. L. CHERMANT, M. COSTER, A. DESCHANVRES and A. IOST, *J. Less-Common Metals* **52** (1977) 177.
15. S. G. SHIN and H. MATSUBARA, in "Sintering Technology," edited by R. M. German, G. L. Messing and R. G. Cornwall (Dekker, New York,1995) p. 157.
16. S. KIM, J.-K. PARK and D. LEE, *Scripta Mater.* **38** (1998) 1563.
17. L. AKESSON, PhD thesis, Royal Institute of Technology, Stockholm, 1982.
18. V. CHABRETOU, O. LAVERGNE, S. LAY, L. PONTONNIER and C. H. ALLIBERT, in Proceedings of Powder Metallurgy World Congress (EPMA, Grenade, 1998) Vol. 4, p. 146.
19. C. H. ALLIBERT, in Proceedings of EuroPM99, Advances in Hard Materials Production (EPMA, Torino, 1999).
20. J. SERRA, "Image Analysis and Mathematical Morphology," Vol. I (Academic Press, London, 1982).

21. J. M. MISSIAEN and S. ROURE, *J. Microsc.* **199** (2000) 141.
22. S.-G. SHI and H. MATSUBARA, in "Sintering Technology," edited by R. M. German, G. L. Messing and R. G. Cornwall (Marcel Dekker Inc., New York,1996) p. 157.
23. H. E. EXNER and H. FISCHMEISTER, *Archiv für das Eisenhüttenwesen* **37** (1966) 417.
24. R. WARREN and B. WALDRON, *Powder Metall.* **15** (1972) 166.
25. O. LAVERGNE, F. ROBAUT, F. HODAJ and C. H. ALLIBERT, *Acta Mater.* **50** (2002) 1683.
26. M. HILLERT, in "Lectures on the Theory of Phase Transformation," edited by H. I. Aaronson (American Institute of Mining, 1975).
27. A. P. GERK and J. J. GILMAN, *Journal of Applied Physics* **39** (1968) 4497.
28. A. EGAMI, in Proceedings of 13th Int. Plansee Seminar, edited by H. Bildstein and R. Eck (Plansee AG, Reutte, 1993) Vol. 3, p. 639.
29. T. TANIUCHI, K. OKADA and T. TANASE, in Proceedings of 14th Int. Plansee Seminar, edited by P. Rödhammer and P. Wilhartitz (Plansee AG, Reutte, 1997) Vol. 2, p. 644.
30. A. JAROENWORALUCK, *J. Mater. Res.* **13** (1998) 2450.
31. S. LAY, S. HAMAR-THIBAULT and A. LACKNER, in Proceedings of 15th Int. Plansee Seminar, edited by G. Kneringer, P. Rödhammer and H. Wildner (Plansee AG, Reutte, 2001) Vol. 2, p. 106.
32. P. WARBICHLER, F. HOFER, W. GROGGER and A. LACKNER, in Proceedings of 15th Int. Plansee Seminar, edited by G. Kneringer, P. Rödhammer and H. Wildner (Plansee AG, Reutte, 2001) Vol. 2, p. 65.
33. R. K. SADANGI, L. E. McCANDLISH, B. H. KEAR and P. SEEGOPAUL, *Int. J. Powder Metall.* **35** (1999) 27.
34. B. WITTMANN, W. D. SCHUBERT and B. LUX, in Proceedings of 15th Int. Plansee Seminar, edited by G. Kneringer, P. Rödhammer and H. Wildner (Plansee AG, Reutte, 2001) Vol. 4, p. 427.
35. M. KUMAZAWA, *Materials Transactions, JIM* **31** (1990) 685.
36. H. S. RYOO and S. K. HWANG, *Scripta Mater.* **39** (1998) 1577.
37. A. SCHÖN, W. D. SCHUBERT and B. LUX, in Proceedings of 15th Int. Plansee Seminar, edited by G. Kneringer, P. Rödhammer and H. Wildner (Plansee AG, Reutte, 2001) Vol. 4, p. 322.
38. Y. WANG, S. LAY and C. ALLIBERT, in Proceedings of European Congress and Exhibition on Powder Metallurgy—PM 2001 (Nice, 2001) p. 2001.
39. J. N. BARBIER and C. BERNARD, in Proceedings of CALPHAD XV (1986).

Received 21 October 2002
and accepted 17 March 2003